

Tip Clearance Investigation of a Ducted Fan Used in VTOL Unmanned Aerial Vehicles—Part II: Novel Treatments Via Computational Design and Their Experimental Verification

Ali Akturk¹

e-mail: akturkali@gmail.com

Cengiz Camci²

Professor of Aerospace Engineering
e-mail: cxc11@psu.edu

Turbomachinery Aero-Heat Transfer Laboratory,
Department Aerospace Engineering,
Pennsylvania State University,
University Park, PA 16802

Ducted fan based vertical lift systems are excellent candidates to be in the group of the next generation vertical lift vehicles, with many potential applications in general aviation and military missions. Although ducted fans provide high performance in many “vertical take-off and landing” (VTOL) applications, there are still unresolved problems associated with these systems. Fan rotor tip leakage flow adversely affects the general aerodynamic performance of ducted fan VTOL unmanned aerial vehicles (UAVs). The current study utilized a three-dimensional Reynolds-averaged Navier-Stokes (RANS) based computational fluid dynamics (CFD) model of ducted fan for the development and design analysis of novel tip treatments. Various tip leakage mitigation schemes were introduced by varying the chordwise location and the width of the extension in the circumferential direction. Reduced tip clearance related flow interactions were essential in improving the energy efficiency and range of ducted fan based vehicles. Full and inclined pressure side tip squealers were also designed. Squealer tips were effective in changing the overall trajectory of the tip vortex to a higher path in radial direction. The interaction of rotor blades and tip vortex was effectively reduced and the aerodynamic performance of the rotor blades was improved. The overall aerodynamic gain was a measurable reduction in leakage mass flow rate. This leakage reduction increased thrust significantly. Experimental measurements indicated that full and inclined pressure side tip squealers increased thrust obtained in hover condition by 9.1% and 9.6%, respectively. A reduction or elimination of the momentum deficit in tip vortices is essential to reduce the adverse performance effects originating from the unsteady and highly turbulent tip leakage flows rotating against a stationary casing. The novel tip treatments developed throughout this study are highly effective in reducing the adverse performance effects of ducted fan systems developed for VTOL UAVs. [DOI: 10.1115/1.4023469]

Introduction

Ducted fan designs require large tip clearances in order to safely operate in VTOL UAVs. The large tip clearance induced flow has a damaging effect on the fan rotor aerodynamic performance. It is also a significant energy loss mechanism in the ducted fans.

This paper describes the development of novel tip treatments for ducted fans used in VTOL UAVs. Ducted fan VTOL UAVs use large tip gaps because of their operating conditions. Large tip clearance flow increases the aerodynamic losses on the fan rotor and diminishes the performance of the ducted fan. Novel tip treatments are aimed to reduce the losses and improve performance.

There have been a limited number of studies about three-dimensional flow structure of leakage vortex in axial flow fans and compressors in open literature [1–6]. Inoue and Kurokamaru et al. [7]

made detailed flow measurements before and behind an axial flow rotor with different tip clearances. In their study, they investigated the clearance effect on the behavior of tip leakage flow. Furukawa and Inoue et al. [8] also investigated breakdown of tip leakage vortex in a low speed axial flow compressor. Reducing tip leakage mass flow rate improves the aerodynamic performance of axial flow fans and compressors. Implementation of treatments in the nonrotating part over the blade tip is also an efficient way of tip leakage flow reduction. References [9] and [10] investigate different casing treatments for axial flow compressors.

A few authors investigated tip treatments in turbomachinery components for tip leakage mass flow reduction. Corsini et al. [11–15] presented the results of a computational study of an axial flow fan using “improved tip concepts.” The first two end plates were with constant and variable thickness distributions while the last two were designed by combining the end plates with a stepped gap on the tip. The investigation was based on a finite element Navier-Stokes solver for the physical interpretation of the detailed 3D leakage flow field. The specific fan performance experiments showed that the improved tip concepts introduced a small performance penalty, but the efficiency curves give evidence of an

¹Currently working in Siemens Energy Inc.

²Corresponding author.

Contributed by International Gas Turbine Institute (IGTI) of ASME for publication in the JOURNAL OF TURBOMACHINERY. Manuscript received November 5, 2012; final manuscript received December 8, 2012; published online September 26, 2013. Editor: David Wisler.

improvement with better peak performance and a wider high efficiency curve toward the rotor stall margin. An aeroacoustic investigation showed a reduction of the rotor aeroacoustic signature.

Wisler [16] presented a study on tip clearance and leakage effects in compressors and fans. He discussed the effect of clearance, duct design, tip treatments, active clearance control, and improving stall margin of rotor blade in his study. He came up with several tip treatment geometries. He tested squealer tip, groove, pressure, and suction side winglet, knife type tip configurations. The most common one of these treatments is the squealer tip obtained by thinning the rotor tip. The main reason for a squealer tip is the reduction of the contact surface during a "rubbing" incidence. A squealer tip has measurable aerodynamic benefits too. Relative to flat tip the deep groove treatment and the pressure surface winglet implementation reduced the leakage.

Akturk and Camci [17] developed novel tip platform extensions for energy efficiency gains and aeroacoustic improvements for a constant rotational speed axial flow fan. They measured three components of velocity at downstream of the fan rotor for five different tip platform extensions, introduced on the pressure side of the fan rotor tip section. They showed that the tip platform extensions proved to be effective swirl reducing devices at the exit of the fan. The magnitude of this reduction is about one-third of the rotor exit velocity magnitude in the core of the passage exit. Their results also showed that the mean kinetic energy of fan exit flow increased due to the increase in mean axial velocity.

Martin and Boxwell [18] tested two ducted fan models that were designed to effectively eliminate the tip leakage. Both models were derived from the baseline (254-mm inner-diameter shroud), which is explained in their previous study [19]. In their first design, they created a notch and fit the propeller inside the notch. In their second design, a rearward-facing step was cut into the inner shroud. The computational analysis resulted in an increase in inlet lip suction and an increase in performance. However, the experimental thrust and power measurements showed no difference in performance of these designs when compared to their baseline duct.

Novel tip platform extensions for aerodynamic and aeromechanic improvements were designed in the current investigation for a ducted fan VTOL UAV in hover condition. Five tip treatments were developed by using numerical solutions of Reynolds-averaged Navier-Stokes equations. Selected computationally developed tip treatments were also experimentally verified in the 559-mm ducted fan test bench. Fan rotor downstream total pressure surveys and force and moment measurements were performed. The main goal of this paper is to develop effective tip treatments for reducing tip leakage flow for large tip gaps used in ducted fans for VTOL UAVs. This paper presents a set of comprehensive ducted fan aerodynamic measurements validating and supporting the computationally developed novel tip treatments named full and partial bump tip extensions, full bump and partial squealer tip extensions, and full squealer and inclined squealer tips in hover condition. A comprehensive assessment and validation of the computational method used in this paper were explained in an accompanying paper by Akturk and Camci [20].

Design Algorithm of Tip Treatments

Computational Method. A three-dimensional computational method can be used to develop novel tip treatments for improving aerodynamic performance of the ducted fan in hover.

Reynolds-averaged Navier-Stokes solutions were obtained for computational analysis by using Ansys-CFX. The computational analysis for the tip treatment development was performed on three different computational domains that are connected. The details of the computational method, computational domain sections, grid implementation, and boundary conditions used in this paper can be found in an accompanying paper by Akturk and Camci [20]. The inlet section includes an inlet lip surface that was considered as a solid wall with a no-slip condition. Atmospheric static pressure was

prescribed on the top surface. On the side surface, an opening type boundary condition was assumed.

The outlet section includes the outer duct surface, circular rods, rotor hub surface, and support structure underneath of the system that are considered as solid walls with no-slip condition. The bottom surface is also treated with no-slip boundary condition. On the side surface, an opening boundary condition is assumed.

The rotating section includes the fan blades, rotor hub region, and shroud surface. The rotating fluid motion at a constant angular velocity is simulated by adding source terms to the Navier-Stokes equations for the effects of the Coriolis force and the centrifugal force. Counterrotating wall velocities are assigned at the shroud surface.

Stationary and rotating regions were subsectional by periodic surfaces. By the help of periodicity, the speed of numerical simulations was increased. The stationary surfaces were divided into four segments, and the rotating region was divided into eight periodic segments. Only one of these segments for each region was used in numerical calculations. The difference in pitch angles of the frames was taken into account in interfaces that are connecting rotating and stationary surfaces. A stage type interface model was used.

The stage model performs a circumferential averaging of the fluxes on the interface surface. This model allows steady state predictions to be obtained for turbomachinery components. The stage averaging at the frame change interface introduces one-time mixing loss. This loss is equal to assuming the physical mixing supplied by the relative motion between stationary and rotating surfaces. General grid interface (GGI) was used for mesh connections between interfaces.

Figure 1 illustrates a view from medium size computational mesh near the squealer and inclined squealer rotor tips. Nondimensional wall distance (y^+) less than 2 was achieved near the shroud, rotor tip, and treatment surfaces.

The numerical simulations for tip treatments were obtained at 2400 rpm rotor speed for hover condition. Calculations were performed using a parallel processing approach. For the parallel processing, the stationary and rotating frames were partitioned via vertex based partitioning with METIS multilevel k-way algorithm. Computations were performed on a cluster having 24 processors. Total processing time was approximately 54.9 h. The flow within

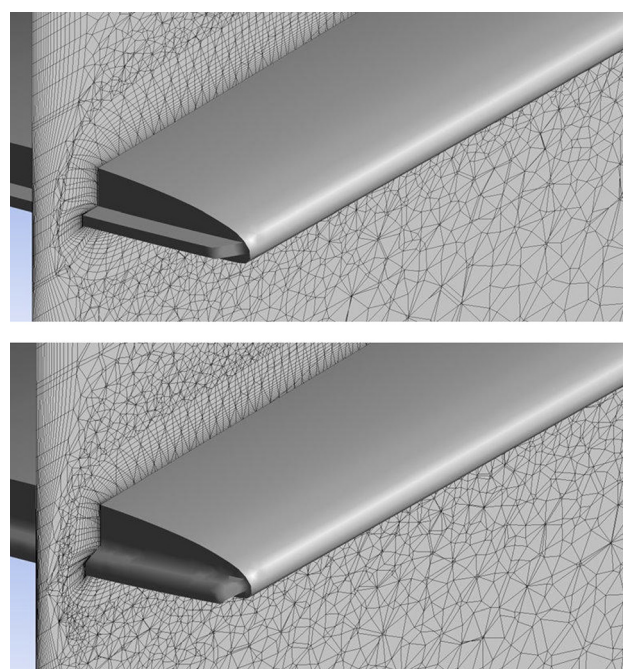


Fig. 1 The near tip computational grid for squealer and inclined squealer rotor tips

the computational domain was initialized as no flow at the free-stream static conditions. The converged solution was achieved approximately within 4500 iterations. The root mean square (rms) residuals of the Navier–Stokes equations were compared for judging convergence.

Blade Tip Constant Circumferential Angle Planes. The visualization planes obtained at constant circumferential angles were generated at the rotor blade tip for a better understanding of the rotor tip region flow. They were all passing from the axis of rotation and drawn at fixed circumferential position (θ). Three of these planes (A, B, and C) were drawn just upstream of the rotor tip and they were separated by 4 deg circumferential angle from each other and plane D. Plane D was drawn at the quarter chord of the tip profile. Planes E, F, G, H, and I were equally distributed near the rotor tip profile by 2 deg circumferential angle increments. Plane I was drawn at the trailing edge.

Constant circumferential angle planes drawn in Fig. 2 are colored with the magnitude of stretched swirling strength. Swirling strength is the imaginary part of complex eigenvalues of velocity gradient tensor. It is positive if and only if there is existence of a swirling local flow pattern and its value represents the strength of swirling motion around local centers. Stretched swirling strength is swirling strength times the product of swirling vector and normal of swirling plane. An increase in this parameter indicates that swirling strength normal to swirling plane is increased.

The quantity color coded in these planes is the velocity stretched swirling strength drawn on the constant circumferential angle planes. The swirling strength shows the magnitude of the out of plane swirling motion. The red color indicates a region that the highest swirling motion is occurring. Planes A, B, and C show swirling strength upstream of the rotor blade. A small amount of swirling motion can be observed in these planes that is related to the tip vortex originating from the previous blade. The positioning of each tip vortex influencing the neighboring blade is clearly shown in Part I of this paper [20]. The vortical field originating from the previous blade tip vortex interacts with the blade tip. This vortical field is divided into two parts as suction side and pressure side parts. The suction side part is integral with the tip vortex of the current blade. The pressure side part interacts with the pressure side of the rotor blade and generates additional loss at the exit plane that is shown in the Flow Field Analysis section of Part I of this paper [20]. The strongest swirling motion starts at the quarter chord of the blade tip measured from the leading edge. Leakage flow tries to pass to the suction side by generating a vortical structure that is visible at plane D. In planes E, F, G, H, and I the path of the released vortical structure from the pressure side corner can be viewed. Once the vortical structure forms, the

strength of it is not as high as the one observed near the pressure side corner seen in plane D. The size of the flow structure dominated by light blue and green zones is increasing when one travels from the leading edge to trailing edge.

Tip Treatment Geometries

Tip leakage flow results in a considerable amount of aerodynamic loss in rotor flow field as discussed in the Flow Field Analysis section of Part I of this paper [20]. One way of reducing tip losses is to use proper tip treatments. The specific tip treatments subject to investigation in this paper include special extensions of rotor tip platform and squealer tips. Both types of tip treatments are widely used in axial flow fans and compressors. Figure 3 shows the tip platform extension concepts and squealer tip concepts that are subject to investigation in this section.

Partial Bump Tip Platform Extension. Effectiveness of partially blocking the pressure side of the fan rotor tip in mitigating tip leakage was explained by Akturk and Camci [17]. It was shown that profiles 1 and 2 that are using partial bump type tip platform extension at the pressure side of the fan rotor tip were the best choices for reducing the effects of tip leakage and improving axial flow velocity at the rotor downstream for the lightly loaded fan rotor. Those two bump profiles had the same thickness with the rotor tip profile at the bump center location. The bump thickness was measured in the circumferential plane at a constant radial position.

The partial bump designed for the current VTOL UAV ducted fan shares the same idea: *reducing the tip leakage flow originating from the pressure side corner of the blade tip*. Computational investigations for the baseline fan rotor with 3.04% tip clearance discussed in Part I of this paper showed that the tip leakage starts

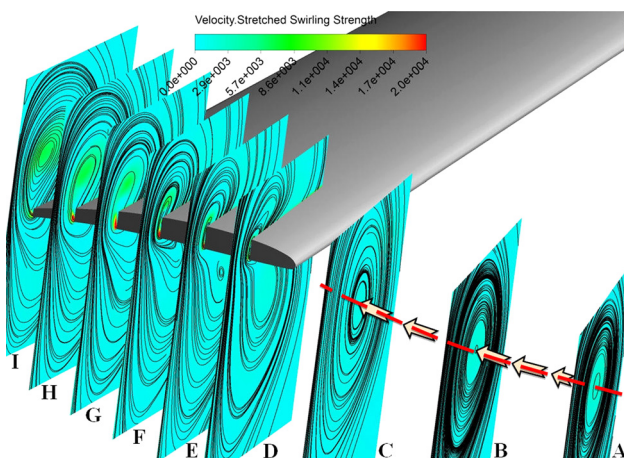


Fig. 2 Blade tip constant circumferential angle planes drawn for baseline rotor tip with 3.04% tip clearance

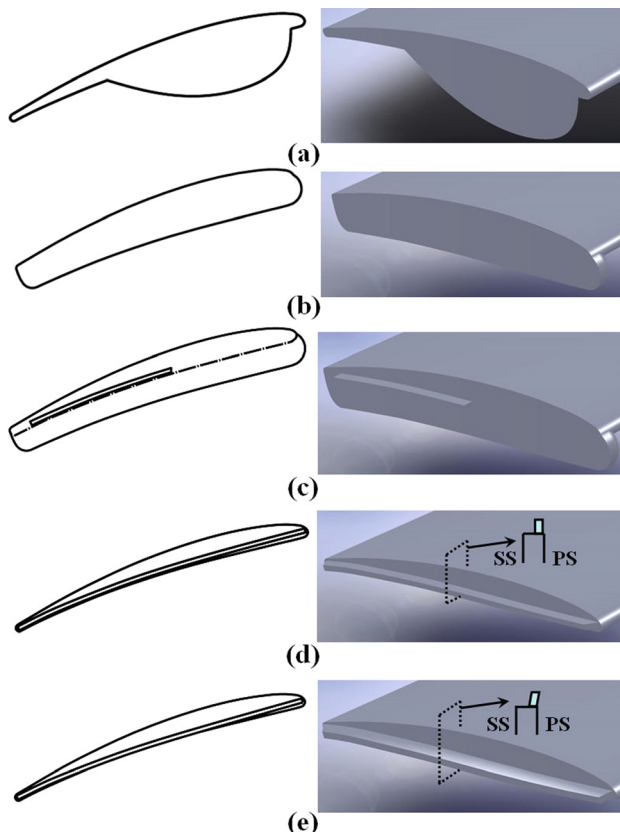


Fig. 3 Tip treatments: (a) partial bump tip platform extension (t.p.e.), (b) full bump t.p.e., (c) full bump and partial squealer t.p.e., (d) full squealer t.p.e., (e) inclined full squealer t.p.e.

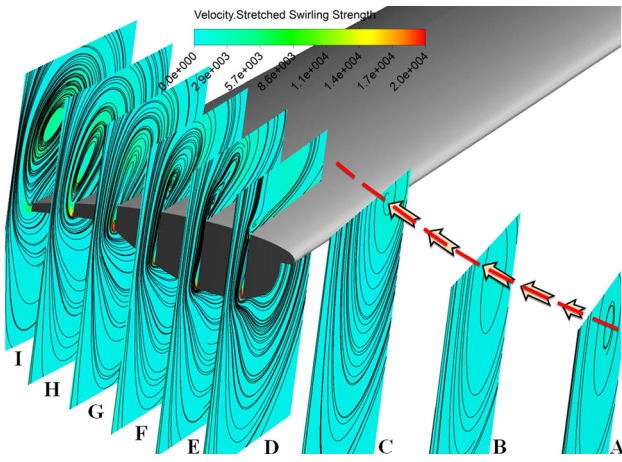


Fig. 4 Blade tip constant circumferential angle planes drawn for “partial bump” tip extension with 3.04% tip clearance

very close to the leading edge of the tip profile. Therefore, a long bump starting from the 5% of chord location and ending at 66.6% tip chord location was designed. The maximum thickness point was selected as the quarter chord (25% of the tip chord) since the highest swirling strength was observed in that location. The maximum thickness of the bump was chosen as “twice the tip chord thickness” at the quarter chord location. Figure 3(a) shows the shape of the bump designed.

Figure 4 shows streamlines and stretched swirling strength contour for partial bump tip extension shown in Fig. 3(a). Planes A, B, and C show tip vortex coming from the previous blade moving radially inward compared to the baseline tip result. The strongest contribution to tip vortex is near plane G. However, a gradual increase in the swirling strength is observed in planes D, E, and F. Tip vortex can be seen in planes G, H, and I with a light green and blue core. The strength of the vortex is slightly higher than the ones obtained for the baseline tip.

Full Bump Tip Platform Extension. Since the leakage flow cannot be effectively blocked by using partial bump tip extension, a full coverage bump tip platform extension was designed to cover the pressure side of the rotor tip completely. The bump starting from the leading edge and ending at the trailing edge of the tip chord was designed. Bump was created by extending pressure side curvature by the airfoil thickness at the quarter chord point of the blade profile. Figure 3(b) shows the shape of the full bump designed.

Figure 5 shows the streamlines and stretched swirling strength contour for full bump tip extension. Planes A, B, and C show tip vortex coming from the previous blade moved more axially compared to the baseline tip and the partial bump result. Full bump tip extension was not sufficient for effectively reducing the leakage flow. Planes D, E, F, G, H, and I show that the strength of the vortical structure was almost same with the baseline rotor tip without a beneficial tip mitigation influence.

Full Bump and Partial Squealer Tip Platform Extension. Since the leakage flow cannot be properly blocked by using only pressure side tip extensions, a combination of a full bump and a partial squealer extension was designed for the region near the trailing edge. Figure 3(c) shows the shape of the combined full bump and partial squealer design. The squealer extension started from 45% chord measured from leading edge and ended at the trailing edge. The height of the squealer was 0.89 mm and thickness was 20% of the tip gap height (1.27 mm for 3.04% tip clearance). The squealer tip was located parallel to the pressure side of the rotor tip and approximately 0.5 mm away from the pressure side.

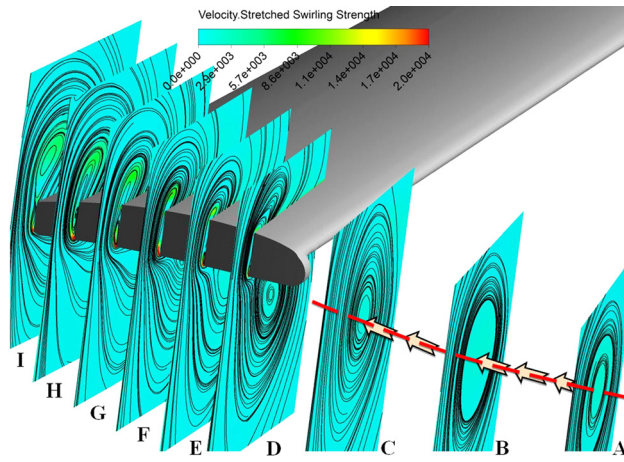


Fig. 5 Blade tip constant circumferential angle planes drawn for “full bump” tip extension with 3.04% tip clearance

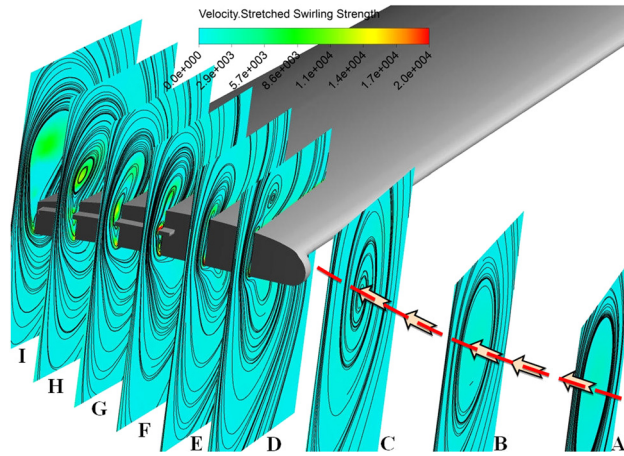


Fig. 6 Blade tip constant circumferential angle planes drawn for “full bump and partial squealer” tip extension with 3.04% tip clearance

Figure 6 shows streamlines and stretched swirling strength contour for a combination of the full bump and squealer tip extension. Planes A, B, and C show tip vortex coming from the previous blade moved more axially compared to the baseline tip and the partial bump result. Full bump and squealer tip extension were not sufficient for blocking leakage flow. Planes F, G, H, and I show the effect of squealer on the flow field near the rotor tip. By the effect of the squealer the swirling strength was increased and tip vortex was moved radially outward, which is a favorable effect. Moving the tip vortex radially out will reduce the interactions between the tip vortex and rotor blade and reduce the losses. However, the combination of full bump and partial squealer increased swirling strength and losses.

Full Squealer Tip Platform Extension. Using a combination of bump and squealer increased turbulence and swirl at the rotor tip as shown in Full Bump and Partial Squealer Tip Platform Extension. A full squealer tip extension was designed to explore its potential as a possible aerodynamic tip mitigation device. Figure 3(d) shows the shape of the full squealer tip designed for this. Squealer extension started from the leading edge of the rotor tip and ended at the trailing edge. The width of the squealer was 0.89 mm and height was 20% of the tip gap height (1.27 mm for 3.04% tip clearance). The squealer tip was located parallel to the pressure side of the rotor tip and 0.5 mm away from pressure side. At the leading edge of the

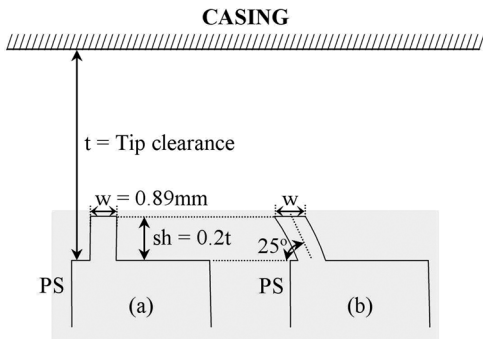


Fig. 7 (a) Full and (b) inclined squealer sketch

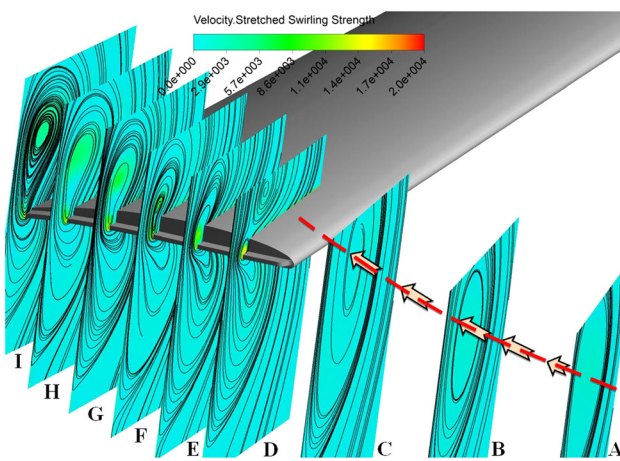


Fig. 8 Blade tip constant circumferential angle planes drawn for "full squealer" tip extension with 3.04% tip clearance

tip profile, it was aligned with the stagnation point of the tip profile. Figure 7 shows a sketch of full and inclined squealers.

Figure 8 shows streamlines and stretched swirling strength contour for full squealer tip extension. Squealer tip extension decreased the strength of swirling at planes D, E, F, G, H, and I. The leakage flow starting from the pressure side rolled up a small vortical structure between the squealer and suction side. After plane F, the vortical structure appeared on the suction side of the rotor tip. Tip vortex started to influence the passage flow beginning plane F. Using a squealer tip also moved tip vortex closer to the shroud and relieved the rotor passage from the adverse effect of tip vortex dominated flow. Thus, interaction of tip vortex and rotor tip was reduced and the rotor tip was loaded better than the baseline rotor tip because of improvements in the passage aerodynamics near the tip.

Inclined Full Squealer Tip Platform Extension. Using the full squealer tip design moved tip vortex toward the shroud. The most important effect of the squealer tip was delaying tip vortex at the rotor tip. The leakage flow was filled into the space between the squealer and suction side of the rotor blade and released on the suction side at the midchord location. Delaying tip vortex release to a chordwise location close to the trailing edge helped to direct tip vortex radially out. Further improvement can be obtained by increasing space between the squealer and suction side of the rotor tip by bending squealer extension toward to pressure side. A fully inclined squealer tip extension was designed by tilting the existing squealer extension about 25 deg toward the pressure side. This in-line squealer design is shown in Figs. 3(e) and 7.

Figure 9 shows streamlines and stretched swirling strength contour for inclined squealer tip extension. The leakage flow originat-

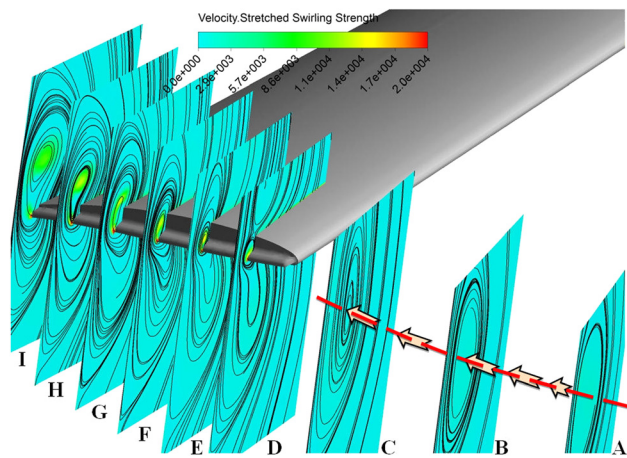


Fig. 9 Blade tip constant circumferential angle planes drawn for "inclined squealer" tip extension with 3.04% tip clearance

ing from the pressure side rolled up a small vortical structure between the inclined squealer and suction side. After plane G, the vortical structure appears near the suction side of the rotor tip. Tip leakage vortex originates starting from plane G and was directed toward the shroud region.

Overall Benefits of Tip Treatments

Overall benefits gained from the tip treatments are analyzed by total pressure improvements in the stationary frame of reference. Table 1 shows computed thrust and ratio of "leakage mass flow rate" to the "fan rotor mass flow rate" for baseline rotor tips for two tip clearances and treated tips. The leakage mass flow rate was calculated on a plane that was defined between the rotor tip and shroud surface.

The result from the two tip clearances, tight (1.71%) and coarse (3.04%), are compared in Table 1. When the tip clearance decreased, the leakage mass flow rate also decreased and thrust was augmented. Decrease in leakage mass flow rate usually implies an increase of overall mass flow rate passing from the duct.

The first two rows of Table 1 present a comparison of both experimental and computational values of ducted fan thrust. The computational thrust results and measured values compare very well at two specific tip clearance values at 1.71% and 3.04%. All of the tip treatments shown in Table 1 are computationally evaluated at the same tip clearance of 3.04%. Aeromechanic and aerodynamic performance improvements provided by tip treatments are also tabulated in Table 1.

Figure 10 compares all of the tip treatments by comparing the spanwise total pressure distributions in the stationary frame of reference. The computationally obtained total pressure distributions are drawn at the same rotor exit plane in which the baseline measurements are performed. This plane is located at about 45.72 mm downstream from the midspan of the fan rotor. The tip clearance value for all computations presented in Fig. 10 is 3.04%.

Because of the increased viscous losses induced at the rotor tip and radial tip leakage flow directed spanwise inward, the performance of partial and full tip platform extensions was lower than the baseline profile. Thrust obtained from the ducted fan was reduced for both treatments. Full tip platform extension combined with a partial squealer effectively reduced the tip leakage flow compared to partial and full tip platform extensions. However, those gains provided by this treatment were not as high as the squealer tip treatments. Full squealer and inclined full squealers were the best performing ones. They improved the aerodynamic performance by moving the tip vortex toward the shroud. The inclined squealer tip increased the thrust provided by the ducted fan by 10.73% at

Table 1 Tip treatments and their computed performance in hover condition at 2400 rpm

Ducted fan performance with baseline fan rotor tip				
	$\frac{\dot{m}_{\text{leakage}}}{\dot{m}_{\text{fan}}} (\%)$	Total thrust (N) (comp.)	Total thrust (N) (exp.)	$\epsilon (\%)$
Baseline rotor tip with 1.71% t.c.	1.81	94.24	92.68	1.68
Baseline rotor tip with 3.04% t.c.	3.41	85.16	83.55	1.93
Baseline rotor tip with 5.17% t.c.	6.35	61.96	67.55	8.27
Ducted fan performance using treated fan rotor tips with 3.04% tip clearance (computational only)				
	$\frac{\dot{m}_{\text{leakage}}}{\dot{m}_{\text{fan}}} (\%)$	D. thrust (N)	R. thrust (N)	Total thrust (N)
				Thrust imp. (%)
Baseline rotor tip	3.41	27.20	57.96	85.16
Partial bump t.p.e.	3.58	26.68	54.06	80.74
Full bump t.p.e.	3.28	26.70	58.20	84.90
Full bump and par. squealer t.p.e.	2.86	27.66	58.68	86.34
Full squealer t.p.e.	2.41	30.50	59.81	90.31
Full inclined squealer t.p.e.	2.35	30.76	63.55	94.31

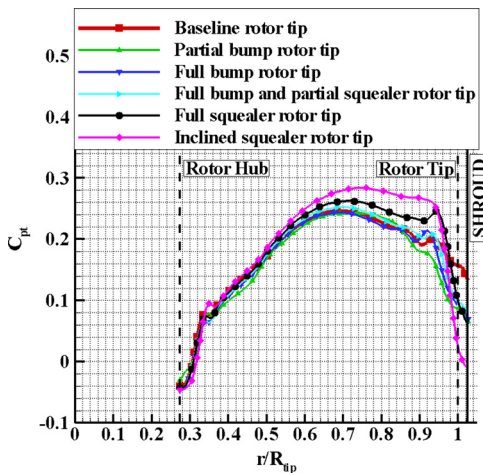


Fig. 10 Comparison of computationally obtained total pressure distributions for all of the tip treatments and baseline rotor tip (3.04% tip clearance)

the hover condition 2400 rpm. It also decreased tip leakage mass flow rate at a considerable rate as shown in Table 1.

Figure 11 shows the streamlines drawn around the tip and mid-span regions for the fan rotor blade with inclined squealer tips. Streamlines are colored by relative velocity magnitude and drawn in the relative frame of reference. The inclined squealer tip directed tip leakage jet toward the casing area as shown in Fig. 11. As a result, the relative velocity magnitudes near the tip region and midspan were increased due to less interaction of leakage jet with the pressure side of the neighboring blade.

Experimental Verification of Computationally Developed Tip Concepts

Experimental Approach. The current study concentrates on the rotor tip section aerodynamic performance improvement by developing novel tip treatments. A computational model was used in the design and analysis of tip treatments as outlined in the Computational Method subsection. Selected treatments were tested using experimental methods. Experimental methods used for this research were total pressure survey at rotor exit and aeromechanic measurements of the ducted fan system.

Fan rotor exit total pressure measurements in the stationary frame of reference were performed by using a Kiel total pressure

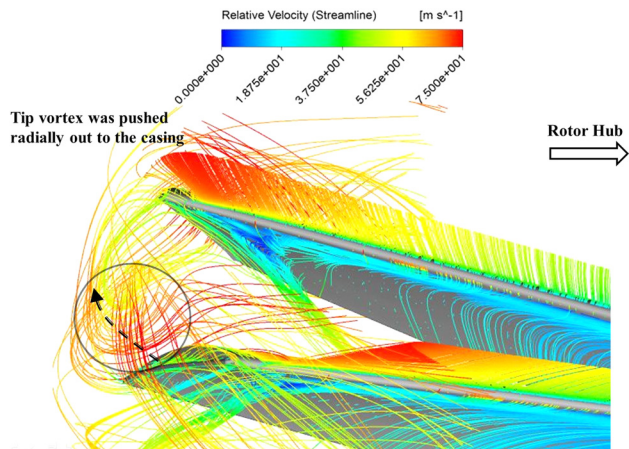


Fig. 11 Streamlines around the inclined squealer rotor blade with 3.04% tip clearance and rotor hub at 2400 rpm

probe. The Kiel total pressure probe having a 5 mm diameter total head was traversed in radial direction using a precision linear transverse mechanism controlled by a computer. The total pressure probe was always located 45.72 mm downstream of the fan rotor exit plane at 50% of blade span (midspan). The Kiel probe was aligned with absolute rotor exit velocity at midspan position. Details of the probe alignment for different spanwise positions are explained in detail in Part I of this paper [20].

Ducted fan aerodynamic research performed in this study requires high accuracy force and moment measurements. The 559-mm diameter fan was equipped with an ATI-Delta six component force and torque transducer. Three components of force and three components of moments were measured. Part I of this paper explains the details of the force and torque measurement details and uncertainties.

Manufacturing Tip Platform Extensions Using a Stereolithography Based Rapid Prototyping Technique. In the Tip Treatment Geometries section the computational analysis was performed for selecting the best tip profile geometries for improving aeromechanic and aerodynamic performance of the system. Squealer and inclined squealer tips both improved thrust of the system while reducing leakage mass flow rate. They also improved fan rotor exit total pressure distribution compared to baseline rotor tips. Three different squealer and inclined squealer designs were selected to be manufactured and experimentally

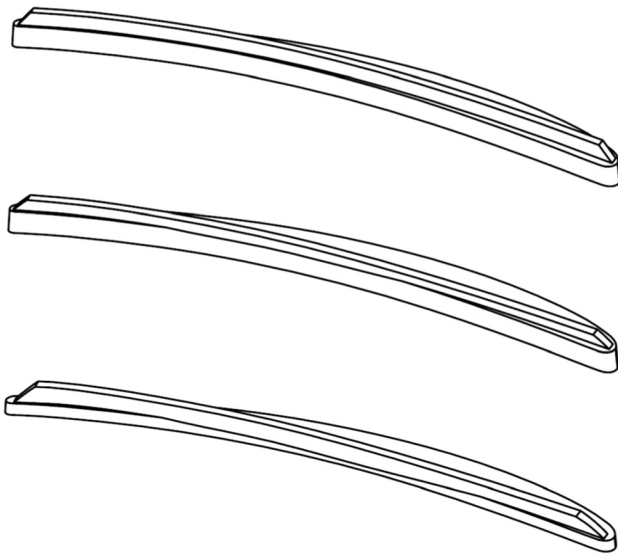


Fig. 12 Squealer and inclined squealer tip extensions designed for SLA manufacturing (a) squealer t.p.e.(3.04% t.c.), (b) inclined squealer t.p.e. (3.04% t.c.), (c) inclined squealer t.p.e. (5.17% t.c.)

tested in hover condition. The baseline tip clearance level for the computational analysis was 3.04%. For the experimental program, squealer and inclined squealer tip treatments were designed for 3.04%. Inclined squealer tip treatment was also tested for 5.17% tip clearance.

Selected tip shapes were designed as an extension to the tip of a baseline fan rotor tip. These extensions conformed to the external contour of the baseline tip section. Figure 12 shows drawings of the extensions designed for the baseline fan rotor tips. The extensions were glued to the top surface of the fan rotor blade using cyanoacrylate that had high viscosity and high impact strength. Figure 13 shows a rotor blade tip that has an inclined squealer tip extension attached to it. Each tip concept tested had its own eight bladed rotor assembly. The tip clearance was measured from the base of the attached tip concept model as shown in Fig. 13.

Experimental Results

Force and Torque Measurements. Force and torque measurements for fan rotors with treated tips were performed in the 559-mm diameter axial flow fan research facility described in Part I of this paper. Figure 14 shows measured thrust coefficient at various rotational speeds. The squealer and inclined tip squealer tip shapes were both augmenting thrust of the system compared to baseline rotor tip shapes. A maximum increase of 9.1% was gained by using the squealer tip shape at 2700 rpm. The maximum increase in thrust gained by using an inclined squealer tip was around 9.6% at 2700 rpm. Compared to computational results, experimental performance of squealer tips was better than computational performance in terms of measured thrust values. Using tip treatments

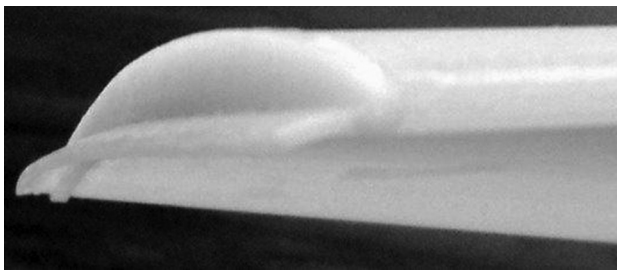


Fig. 13 Inclined squealer t.p.e. applied to the rotor blade (5.17% tip clearance)

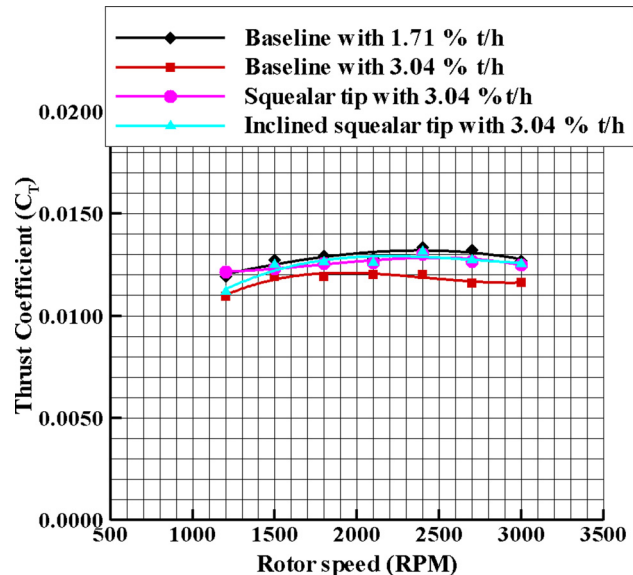


Fig. 14 Measurements of thrust coefficient versus rotational speed for the rotor with squealer and inclined squealer tips at 3.04% tip clearance

improved performance of the baseline rotor tips with 3.04% tip clearance such that the fan rotor with treated tips at the same tip clearance (3.04%) performed almost as well as the baseline fan rotor performance having a tighter tip clearance (1.71%), without any tip treatment. These comparisons are based on measured thrust in the 559-mm diameter ducted fan research facility. The height of the squealer tips used in this study was always one-fifth of the effective clearance t measured between the casing surface and the base platform of the blade tip.

Figure 15 illustrates the aeromechanic performance of an inclined squealer at 5.17% tip clearance compared to baseline rotor at the same clearance. When treatments were used with larger clearance, the improvements obtained were better. Total improvement in thrust was 15.9% at 2700 rpm. Performance of the baseline rotor tips at 5.17% tip clearance was enhanced so that they are almost performing like the 3.04% tip clearance baseline rotor, without any tip treatment.

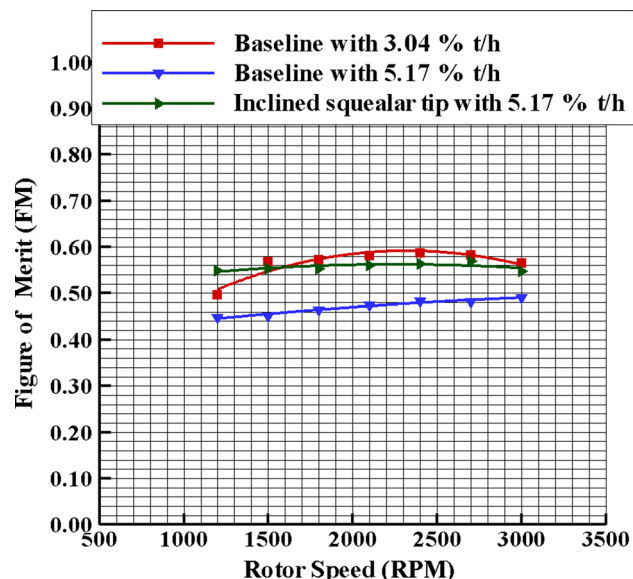


Fig. 15 Measurements of thrust coefficient versus rotational speed for rotor with squealer and inclined squealer tips at 5.17% tip clearance

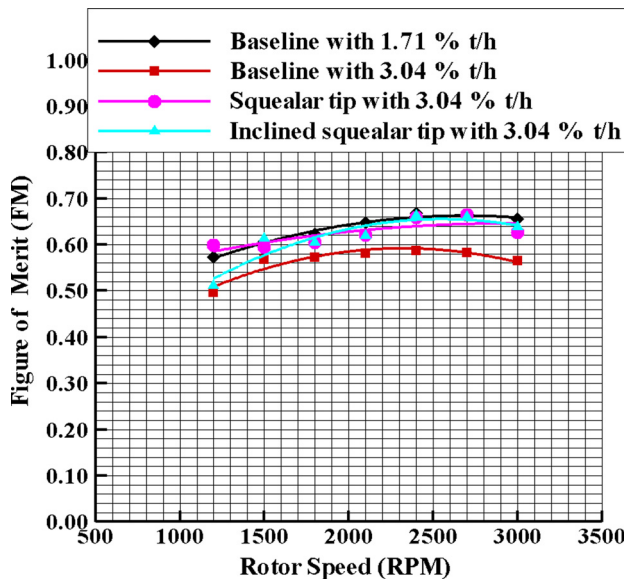


Fig. 16 Measured figure of merit versus rotational speed for rotor with squealer and inclined squealer tips at 3.04% tip clearance

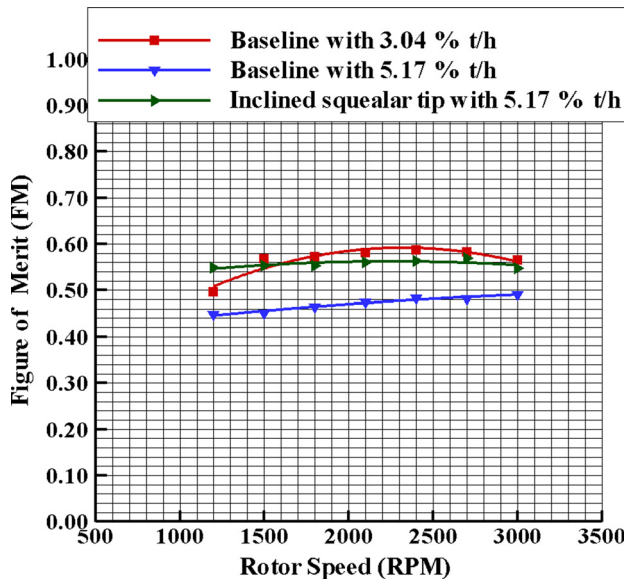


Fig. 17 Measured figure of merit versus rotational speed for rotor with squealer and inclined squealer tips at 5.17% tip clearance

Figures 16 and 17 illustrate the measured figures of merit plotted against the rotational speed of the fan rotor. Squealer and inclined squealer rotor tips increased hover efficiency compared to baseline rotor tips. Treated tip shapes at 5.17% tip clearance performed better than 3.04% tip clearance (no tip treatments).

Total Pressure Measurements. Aerodynamic performance of the ducted fan with squealer rotor tips was assessed by fan rotor exit total pressure measurements at hover condition. Figure 18 shows total pressure coefficient measured at fan rotor downstream from rotor hub to the shroud. It should be noted that there was almost no change in total pressure coefficient by using treated tips when $r/R_{tip} \leq 0.35$. Total pressure at the fan rotor exit plane was increased by using squealer and inclined squealer tip designs at 3.04% tip clearance. Since the tip vortex that is originating from the rotor tip pressure side is repositioned by squealer and inclined squealer tips as mentioned in the Tip Treatment Geometries and

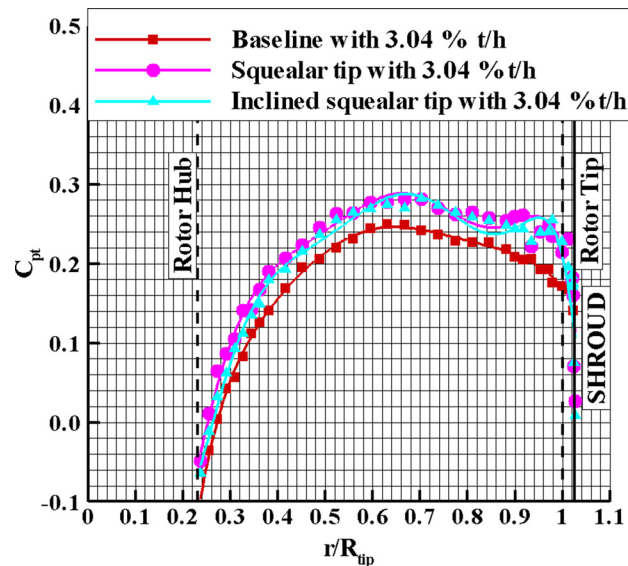


Fig. 18 Total pressure measured at downstream of the rotor at 2400 rpm for squealer tips with 3.04% tip clearance

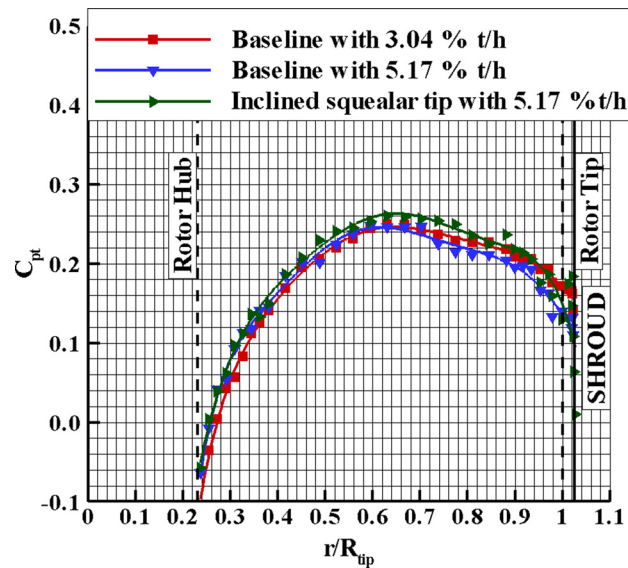


Fig. 19 Total pressure measured at downstream of the rotor at 2400 rpm for squealer tips with 5.17% tip clearance

Overall Benefits of Tip Treatments sections, total pressure distribution at the rotor tip where $r/R_{tip} \geq 0.3$ was enhanced. A significant portion of the blade span above $r/R_{tip} \geq 0.3$ produced a measurably higher total pressure as shown in Fig. 18. The total pressure augmentation from the tip treatments were particularly effective near the blade tip where $r/R_{tip} \geq 0.85$. For the larger tip clearance 5.17% (Fig. 19), using an inclined squealer tip also improved the total pressure distribution near the rotor tip region and performed better than the smaller tip clearance baseline tip performance at 3.04%.

Conclusions

This paper presents a set of comprehensive ducted fan aerodynamic measurements validating and supporting the computationally developed novel tip treatments. The new tip treatments are referred as full and partial bump tip extensions, full bump and partial squealer tip extensions, and full squealer and inclined squealer tips.

The losses generated were highly related to the tip vortex traveling direction and trajectory. If the tip vortex traveled radially inward, then the losses related to the blockage effect influenced a larger portion of the blade span and the rotor tip stall was more pronounced.

The current study used squealer heights that had a total height of one-fifth of the effective clearance t between the base platform and the casing. A full squealer rotor tip was effective in changing the direction of the tip vortex. The tip vortex was pushed radially out to the casing area. The computational results showed that the squealer tip successfully blocked the tip vortex between leading edge and midchord of the rotor tip profile.

An inclined full squealer tip was also conceived to move tip vortex origination location closer to the trailing edge. This was achieved by allocating more space to the tip vortex to fill between squealer and suction side of the rotor tip.

Overall aeromechanic performance gains obtained by using tip platform extensions were assessed from computations. Pressure side tip platform extensions reduced thrust obtained from the ducted fan.

The best performing profiles were full and inclined full squealer extensions. Both experimental measurements and computations confirmed this observation. Full squealer tip extension increased thrust of the ducted fan by 6.04% and reduced the leakage mass flow rated by 29.3% compared to the baseline rotor tips. Inclined squealer tips increased the thrust by 10.73% while reducing the leakage mass flow rate by 31.0%.

Experimental investigation was also performed by manufacturing squealer and inclined squealer tip extensions for 3.04% tip clearance and inclined squealer tip extensions for 5.17% tip clearance. Solid models of tip extension pieces originally developed for computational purposes were directly used to manufacture experimental tip treatment models in a rapid prototyping process.

Aeromechanic and aerothermodynamic measurements showed that using full inclined squealer tips with 5.17% tip clearance is equivalent to working with a 3.04 tip clearance baseline rotor.

The squealer and inclined squealer tips at 3.04% tip clearance also improved performance of the fan rotor. This operation was equivalent to working with a baseline rotor at 1.71% tip clearance. This feature of the tip treatments allows using treated rotor blades at larger clearances while performing as well as operating at much smaller clearances.

The novel tip treatments filling one-fifth of the effective gap between the tip platform and the casing can easily be manufactured out of attachable and flexible materials for VTOL UAV fan implementation. The current state-of-the-art in stereolithography manufacturing allows the rapid production of the proposed tip treatments out of materials such as rubber or other flexible plastic materials of resilient character.

While the flexible tip treatments improve ducted fan thrust and reduce tip clearance leakage mass flow rate, they can be quickly replaced in case of a rubbing incident during field operation.

Acknowledgment

The authors acknowledge the financial support provided by The Pennsylvania State University Vertical Lift Center of Excellence

(VLRCOE) and National Rotorcraft Technology Center (NRTC) (Under U.S. Army Research Office Grant No. W911W6-06-2-0008). They wish to thank Ozhan Turgut for his support throughout this effort. They are also indebted to Mr. Harry Houtz for his technical support.

References

- [1] Lee, G. H., Baek, J. H., and Myung, H. J., 2003, "Structure of Tip Leakage in a Forward-Swept Axial-Flow Fan," *Flow Turbul. Combust.*, **70**, pp. 241–265.
- [2] Jang, C.-M., Furukawa, M., and Inoue, M., 2001, "Analysis of Vortical Flow Field in a Propeller Fan by LDV Measurements and LES—Part I: Three-Dimensional Vortical Flow Structures," *ASME J. Fluid. Eng.*, **123**(4), pp. 748–754.
- [3] Jang, C.-M., Furukawa, M., and Inoue, M., 2001, "Analysis of Vortical Flow Field in a Propeller Fan by LDV Measurements and LES—Part II: Unsteady Nature of Vortical Flow Structures Due to Tip Vortex Breakdown," *ASME J. Fluid. Eng.*, **123**(4), pp. 755–761.
- [4] Storer, J. A., and Cumpsty, N. A., 1991, "Tip Leakage Flow in Axial Compressors," *ASME J. Turbomach.*, **113**, pp. 252–259.
- [5] Lakshminarayana, B., Zaccaria, M., and Marathe, B., 1995, "The Structure of Tip Clearance Flow in Axial Flow Compressors," *ASME J. Turbomach.*, **117**, pp. 336–347.
- [6] Matzgeller, R., Bur, P., and Kawall, J., 2010, "Investigation of Compressor Tip Clearance Flow Structure," Proceedings of ASME Turbo Expo 2010: Power for Land, Sea and Air, Glasgow, UK, June 14–18, *ASME* Paper No. GT2010-23244.
- [7] Inoue, M., Kuromaru, M., and Furukawa, M., 1986, "Behavior of Tip Leakage Flow Behind an Axial Compressor Rotor," *ASME J. Gas Turb. Power*, **108**, pp. 7–14.
- [8] Furukawa, M., Inoue, M., Saik, K., and Yamada, K., 1999, "The Role of Tip Leakage Vortex Breakdown in Compressor Rotor Aerodynamics," *ASME J. Turbomach.*, **121**, pp. 469–480.
- [9] Fujita, H., and Takata, H., 1984, "A Study on Configurations of Casing Treatment for Axial Flow Compressors," *B. JSME*, **27**, pp. 1675–1681.
- [10] Moore, R. D., Kovich, G., and Blade, R. J., 1971, "Effect of Casing Treatment on Overall and Blade-Element Performance of a Compressor Rotor," NASA, Tech. Rep. TN-D6538.
- [11] Corsini, A., Perugini, B., Rispoli, F., Kinghorn, I., and Sheard, A. G., 2006, "Investigation on Improved Blade Tip Concept," *ASME* Paper No. GT2006-90592.
- [12] Corsini, A., Rispoli, F., and Sheard, A. G., 2006, "Development of Improved Blade Tip Endplate Concepts for Low-Noise Operation in Industrial Fans," Proceedings of Conference on Modeling Fluid Flows CMMF06.
- [13] Corsini, A., Perugini, B., Rispoli, F., Kinghorn, I., and Sheard, A. G., 2007, "Experimental and Numerical Investigations on Passive Devices for Tip-Clearance Induced Noise Reduction in Axial Flow Fans," *Proceedings of the Institution of Mechanical Engineers, Part A*, **221**(5), pp. 669–681.
- [14] Corsini, A., Perugini, B., Rispoli, F., Sheard, A. G., and Kinghorn, I., 2007, "Aerodynamic Workings of Blade Tip End-Plates Designed for Low-Noise Operation in Axial Flow Fans," *ASME* Paper No. GT2007-27465.
- [15] Corsini, A., Rispoli, F., and Sheard, A. G., 2010, "Shaping of Tip End-Plate to Control Leakage Vortex Swirl in Axial Flow Fans," *ASME J. Turbomach.*, **132**(3), p. 031005.
- [16] Wisler, D., 1985, "Tip Clearance Effects in Axial Turbomachines," Von Karman Institute for UID Dynamics Lecture Series, VKI LS 1985-05, April 15–18.
- [17] Akturk, A., and Camci, C., 2010, "Axial Flow Fan Tip Leakage Flow Control Using Tip Platform Extensions," *ASME J. Fluids Eng.*, **132**(5), p. 051109.
- [18] Martin, P. B., and Boxwell, D. A., 2005, "Design, Analysis and Experiments on a 10-Inch Ducted Rotor VTOL UAV," American Helicopter Society (AHS) International Specialists Meeting on Unmanned Rotorcraft: Design, Control and Testing, Chandler, AZ, January 18–20.
- [19] Martin, P., and Tung, C., 2004, "Performance and Flowfield Measurements on a 10-Inch Ducted Rotor VTOL UAV," 60th Annual Forum of the American Helicopter Society, Baltimore, MD, June 7–10.
- [20] Akturk, A., and Camci, C., 2011, "Tip Clearance Investigation of a Ducted Fan Used in VTOL UAVs—Part I: Baseline Experiments and Computational Validation," Proceedings of ASME Turbo Expo 2011: Power for Land, Sea and Air, *ASME* Paper No. GT2011-46356.